Available online at www.eccomasproceedia.org
Eccomas Proceedia COMPDYN (2021) 387-397

ECCOMAS
Proceedia

COMPDYN 2021
8th ECCOMAS Thematic Conference on
Computational Methods in Structural Dynamics and Earthquake Engineering
M. Papadrakakis, M. Fragiadakis (eds.)
Streamed from Athens, Greece, 28 - 30 June 2021

NUMERICAL MODELLING OF BONDED BRICKWORK UNDER CYCLIC COMPRESSION LOADING

Mohammad Asad[1], Tatheer Zahra[1], and Julian Thamboo[2]
[1] School of Civil and Environmental Engineering, Queensland University of Technology,
4000, Brisbane, Australia
m.asad@qut.edu.au, t.zahra@qut.edu.au
[2] Department of Civil Engineering, South Eastern University of Sri Lanka,
32360 Oluvil, Sri Lanka
jathamboo@seu.ac.lk

Abstract

Bonded brickwork as loadbearing walls is widely found in the heritage structures worldwide. The bonded brickwork consists of two or more bricks in the thickness direction which causes them to behave differently to single leaf walls which are the basis of masonry design guidelines. The evaluation of bonded masonry structures under dynamic seismic actions therefore requires appropriate numerical modelling techniques accounting for the cyclic loading. Subsequently, a simplified 3D mesoscale numerical model has been developed in this paper to analysis different thicknesses of bonded brickwork under cyclic compression. Each masonry brick was defined using 3D solid elements with 8 nodes and 24 degree of freedom (DOF) representing an enlarged brick consists of a full-scale brick enveloped by half thickness of the mortar bedding layer all around. These masonry bricks were arranged in multiple layers using zero thickness cohesive interface elements to simulate the bond behaviour under shear, tension, and compression actions. A plasticity-based damage constitutive model to represent the damage in the masonry bricks under cyclic compression loading was employed. A threshold strain level was used to enact the element deletion technique for initiating the brittle crack opening in the masonry units. Whereas the joint interface failure between the masonry units was defined using a cohesive model represented by a simple bi-linear traction-separation constitutive law exhibiting an initial linear elastic behaviour at the interface followed by the initiation of the damage and evolution until the surface bonding degradation. The robustness of the developed model under cyclic compression loading has been proven by validating the test data presented for the clay brick selected to construct 9 masonry wallettes of single, double and triple brick thicknesses. The failure modes, cyclic stress-strain curves and stiffness degradation have been studied.

ISSN:2623-3347
Peer-review under responsibility of the organizing committee of COMPDYN 2021.
doi:10.7712/120121.8492.19213

Keywords: *Brickwork; Clay brick; Cyclic Compression; Numerical Modelling; Element deletion; Damage model; Cohesive Zone model*

1 INTRODUCTION

Bonded masonry is invariably used as loadbearing elements in structures and the compressive strength characteristics of this masonry are of prime importance in the design of new and assessment of existing masonry structures. Subsequently, plenty of research efforts have been put in place to comprehend the compressive strength characteristics of various masonry assemblies in the past [1-4]. However, most of the studies in the past were dedicated to determining the monotonic compressive strength properties of masonry, where only limited studies were dedicated to understand the cyclic compression characteristics of masonry, which are needed to assess the performance of masonry elements against seismic or dynamic actions. Moreover, the non-loadbearing masonry infill walls in reinforced concrete or steel frames are also considered to act as diagonal compression struts under in-plane actions [5-6], thus analysing such infill frames under dynamic actions need cyclic compression properties of masonry.

The limited experimental studies on the cyclic compression behaviour of bonded masonry revealed that the characteristics of masonry under cyclic compression are different to monotonic compression in terms of the attainment of strength and deformation characteristics [7-9], where relatively low compressive strength and considerably larger deformation were depicted under cyclic compression than the monotonic loading. As a result of lack of cyclic compression experimental data on various assemblies, the development of constitutive models for masonry under cyclic compression was generally derived from the studies on concrete under cyclic compression [10-12]. While there are some similarities on the general characteristics between the masonry and concrete under cyclic compression, the damage evolution under cyclic compression is greatly different to concrete due to the anisotropic nature and interfacial incompatibility between unit and mortar in masonry. Recently, Thamboo et al. [13] compared the predictability of cyclic compression behaviour of the existing masonry models with the available experimental data and highlighted that most of the models were not able to predict one or other cyclic compression characteristics such as envelop response, plastic strain, unloading and reloading paths accurately. Nonetheless, experimental studies are not always viable to develop constitutive models for masonry under cyclic compression, owing to the diversity of masonry assemblies exist and difficulty in carrying out the cyclic testing. Therefore, numerical assessment of masonry under cyclic compression is a prudent solution.

Although plenty of progresses have been made to develop numerical methods to assess the masonry at different scales (micro, meso and macro) under various loading conditions [14-16], no systematic methodologies were developed to evaluate the cyclic compression behaviour of masonry in the past. Obviously, micro modelling technique is the most appropriate approach to assess the various assemblies of masonry under a localised loading situation. As an alternative to complex micro-modelling, simplified micro modelling of bonded masonry can save computational effort and avoid complexity of modelling additional mortar joints in the thickness of bonded brickwork. In this technique, mortar thickness is omitted by expanding the bricks into an equivalent masonry material which are joined to make assemblies of various patterns through zero thickness interfaces. Simplified micro-modelling based numerical assessment under cyclic compression could predict the characteristics of masonry reasonably,

especially in terms of damage evolution and localised stress-strain responses as it has been used earlier for the monotonic loading conditions [17-19].

This paper provides the details of a simplified 3D micro-scale modelling technique to assess the characteristics of bonded masonry under cyclic compression. The rationality of the developed modelling technique and outcome under cyclic compression loading simulation have been validated against the results from the experimental campaign carried out previously to assess the cyclic characteristics of bonded brickworks by the third author. Subsequently, Section 2 explains the simplified micro-modelling based numerical procedures established to simulate the cyclic compression behaviour of masonry. The validation of the numerical method against the experimental data is described in Section 3. Finally, the key conclusions derived from the study are mentioned in Section 4.

2 NUMERICAL MODELLING TECHNIQUE

An explicit finite element modelling method was developed to simulate the bonded brickwork response under cyclic compression loading. A simplified 3D mesoscale homogenised material model was adopted to analyse different thicknesses of bonded brickwork under cyclic compression. The material and contact non-linearities were incorporated in this model, and the parameters were calibrated using the datasets of the single brick thick wallette test specimens. Figure 1 shows the developed FE model of the brickwork constructed of single, double and triple bricks in their thickness.

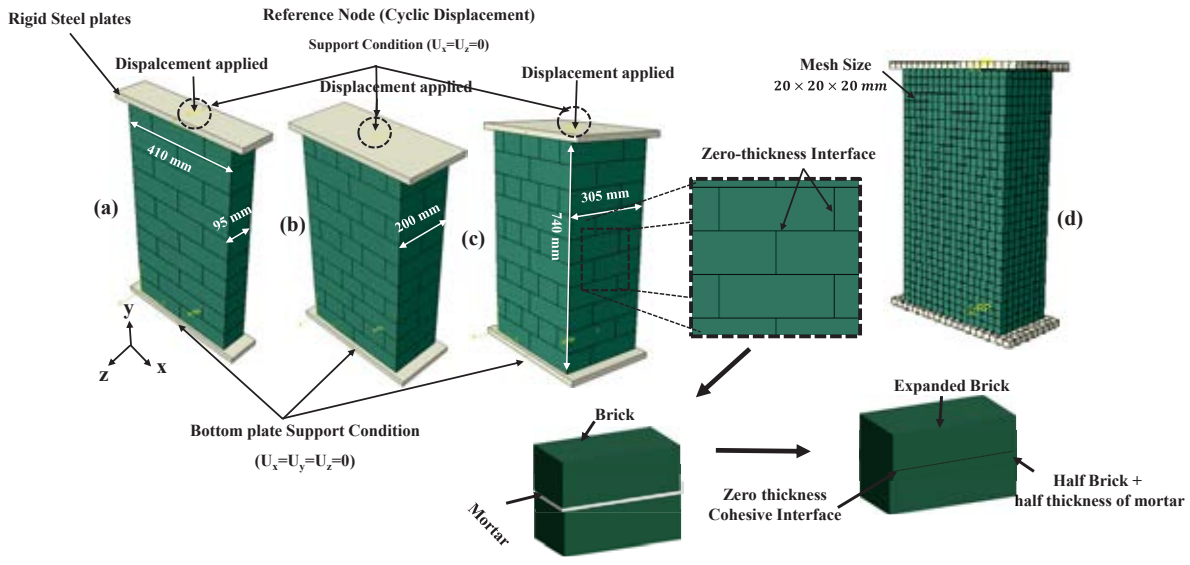

Figure 1: Wallettes model details (a) Single brick (b) Double brick (c) Triple brick with detail of expanded bricks and (d) Mesh size

2.1 Geometry Details

In the simplified 3D mesoscale homogenised numerical modelling method, the homogenised units were modelled using 3D solid elements (C3D8R) with 8 nodes and 24 degrees of freedom. The selected mesh size (shown in Figure 1(d)) was 20 mm × 20mm × 20mm based on the mesh sensitivity analysis performed in [17]. The brick size representing an enlarged brick consists of full-scale brick enveloped by half-thickness of the mortar bedding layer all around,

was modelled as shown in Figure 1. These masonry bricks were arranged in multiple layers using zero thickness cohesive interface elements to simulate the bond behaviour under shear, tension, and compression actions. The sizes of single, double and triple brick thick brickwork samples were 410 (L) × 740 (H) × 95 (T) mm, 410 (L) × 740 (H) × 200 (T) mm, and 410 (L) × 740 (H) × 305 (T) mm, respectively. Loading plates were also modelled to distribute the compressive load uniformly over the specimens and to restrain the specimens against displacement from the bottom.

2.2 Material properties and constitutive model of expanded bricks

A plasticity-based damage constitutive model to represent the damage in the masonry bricks under cyclic compression loading was employed. The concrete damage plasticity (CDP) model in-built in ABAQUS was used to simulate homogenised brick and mortar behaviour. This model can predict two main failure modes: tensile cracking and compression crushing. Beyond the failure limit, the formation of minor and major cracks were represented with a softening stress-strain response, as shown in Figure 2. The stress-strain and other material data were taken from the experimental results of Thamboo & Dhanasekar [20], which were used in the calibration and validation of model results. A threshold strain level was used to enact the element deletion technique for initiating the brittle crack opening in the masonry units. The elastic modulus of the expanded clay bricks was input as 200 MPa. The Poisson's ratio was kept as 0.18 as was observed from the experiments [20]. In addition, the CDP model requires five main parameters: dilation angle (ψ) to account for the volume change caused by the inelastic behaviour of bricks, flow potential eccentricity (e) that defines the rate at which the hyperbolic flow potential approaches its asymptote, the ratio of the biaxial compressive strength of the material to its uniaxial compressive strength ratio (f_{b0}/f_{c0}), shape factor (K_c) which is the ratio of the tensile to the compressive meridian for describing the shape of the yield surface and viscosity (μ) that represents the relaxation time of the visco-plastic system, and is used for the visco-plastic regularisation. More details of these parameters can be found in [21]. The assigned CDP parameters are given in Table 1.

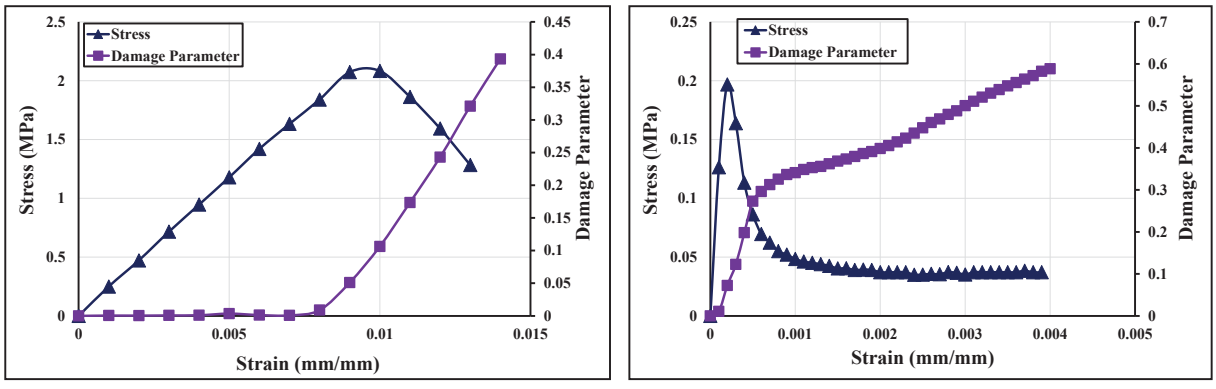

Figure 2: Stress-strain curve with damage properties of clay brick for CDP material model (a) Compression and (b) Tension

Parameter	Magnitude
Dilation angle (ψ)	30^0
Eccentricity (e)	0.1
Strength ratio (f_{b0}/f_{c0})	1.16
Shape factor (K_c)	0.66
Viscosity (μ)	0.001

Table 1: CDP model parameters for expanded bricks

2.3 Zero thickness interface: cohesive zone model

The zero-thickness interface between the homogenised expanded bricks was simulated using the cohesive zone model as shown in Figure 3(a). The interaction between the bricks was modelled using the simple bi-linear separation constitutive law, as shown in Figure 3 (b). The traction law is graphically represented using the traction force (τ) resulted in the opening displacement (δ). The interface allowed a damage initiation based on the threshold value which is followed by damage evolution until complete degradation of the surface bonding. The interface's elastic behaviour relates the normal and the shear (tractions) to the normal and shear displacements (separation) across the interface.

The normal stiffness matrix (K_n) is directly related to the thickness of the adhesive (cement) properties and the stiffness of the mortar (bedding layer). To evaluate the normal stiffness at the interface, a mathematical expression used for this relation is given in Equation (1).

$$K_n = \left(\frac{1}{\frac{t_{mortar}}{E_{mortar}} + \frac{t_{ad}}{E_{ad}}} \right) \tag{1}$$

Where t_{ad} represents the thickness of the adhesive found in the cement [22], t_{mortar} is the thickness of the mortar bedding layer and the E_{mortar} [20] and E_{ad} [22] are the young modulus of the mortar and the adhesive, respectively.

Similarly, the shear stiffness matrix (K_{ss} and K_{tt}) at the interface is mathematically expressed as shown in Equation (2).

$$K_0 = K_{ss} = K_{tt} = \left(\frac{1}{\frac{t_{mortar}}{G_{mortar}} + \frac{t_{ad}}{G_{ad}}} \right) \tag{2}$$

Where, G_{ad} and G_{mortar} are defined as the shear moduli of adhesion and mortar, respectively. The input values for the interface modelling are provided in Table 2.

The damage initiation in the interface was assumed to occur when a quadratic traction factors involving the combined normal stress and shear stress ratio reached to the value of 1 as shown in Equation (3). These criteria can be represented as

$$\left\{ \frac{\langle \sigma_n \rangle}{\sigma_n^0} \right\}^2 + \left\{ \frac{\langle \tau_s \rangle}{\tau_s^0} \right\}^2 + \left\{ \frac{\langle \tau_t \rangle}{\tau_t^0} \right\}^2 = 1 \tag{3}$$

Where σ_n is the cohesive tensile and the τ_s and τ_t are the shear stresses of the interfaces and n,s and t refers to the direction of the stress component as shown in Figure 3(c).

However, the interface damage evolution was expressed in terms of fracture energy release as shown in Equation (4).

$$G_n^c + (G_s^c - G_t^c)\left(\frac{G_s + G_t}{G_n + G_s + G_t}\right)^{\eta} = G^c \quad (4)$$

Where, G is the fracture energy; the superscript c represents the critical fracture energy and the dependency of the fracture energy η is a material parameter (Benzeggagah & Kenane [23]. The Benzeggagah- Kenane fracture criterion defines the critical fracture energies when the deformation along the first and the second shear directions are same. The properties of the zero-thickness interface to account for cohesion, traction separation law and friction are listed in Table 2.

Parameter	Magnitude
Normal stiffness, K_n N/mm^3)	28
Shear stiffness, K_{ss} and K_{tt} (N/mm^3)	32
Friction coefficient	0.6
Maximum tensile stress, σ_n^0 (MPa)	0.68
Maximum shear stress, τ_s^0 and τ_t^0 (MPa)	0.82

Table 2: Mechanical properties of cohesive interfaces

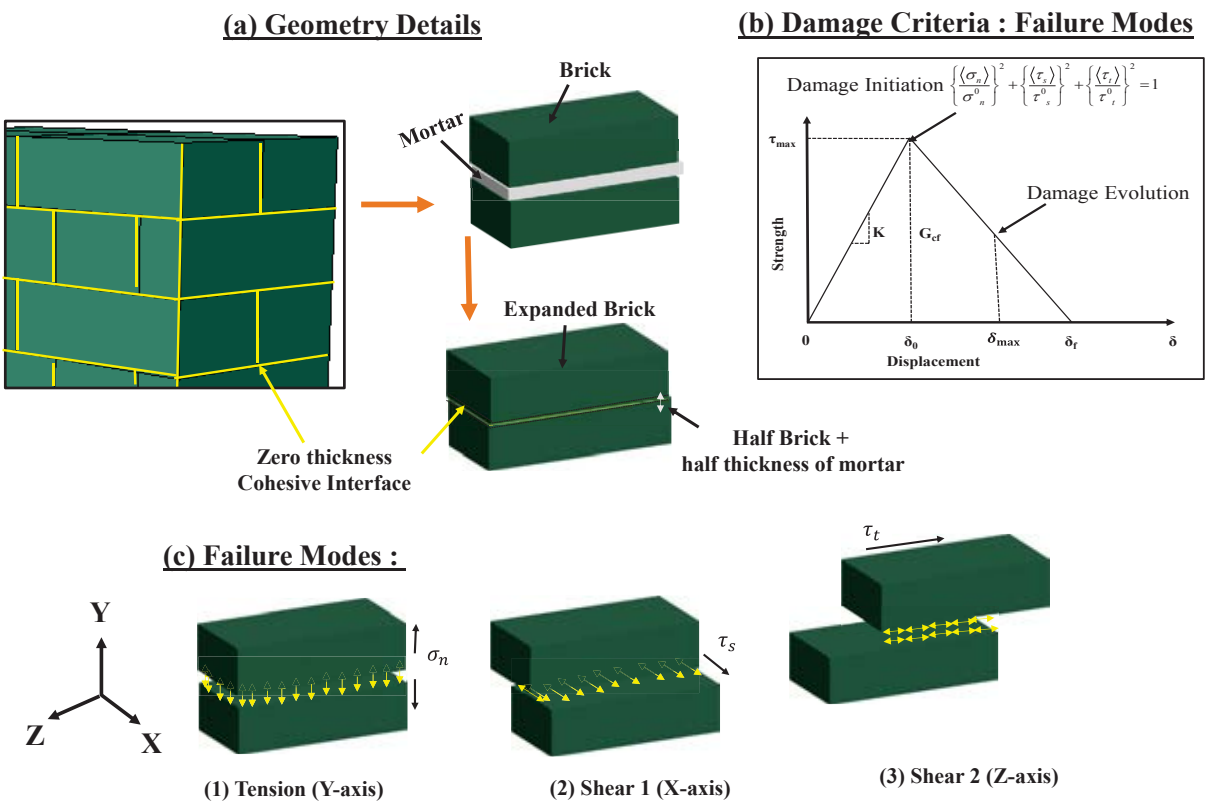

Figure 3: Zero thickness Cohesive Interface model details (a) geometry details of zero-thickness interface (b) damage criteria at the interface (c) failure modes at the interface

3 VALIDATION RESULTS

This section presents the validation of the FE model using the experimental results of single, double and triple brick thick wallettes under cyclic compression loading presented in [20]. The validation includes the failure modes of bonded brickwork walletes, stress-strain curves comparison with the experimental results and the strain variation in the region of damage.

3.1 Details of experimental programme

The experimental investigation on the cyclic response of the masonry wallettes was studied by the authors in the previous study [20]. The tested bonded brickwork samples in this experimental programme were constructed using clay bricks. The material properties and geometrical descriptions of types of bonded brickworks are presented in Figures 1 and 2. The properties of clay bricks varied mainly due to the manufacturing process depending on the controlled and uncontrolled firing in the kiln. However, the bricks used in this study with low strength and modulus of rupture are very common in practice in many developing countries. These bricks also have resemblance to the brick types mainly found in the historical masonry structures. In total, nine bonded brickwork wallettes were constructed with three different thickness (single, double, and triple) to assess their cyclic compression behaviour. The wallettes were built and tested according to BS EN 1052-1 provisions and loaded under the cyclic displacement-controlled protocol. The thickness of the mortar was restricted to 10 mm with the help of an experienced mason. The constructed masonry wallettes were air cured for 28 days under an ambient temperature of 34^{o}C.

The wallettes were tested in a 1000 kN capacity servo-controlled Universal Testing Machine (UTM). A 5 mm thick plywood was used between the top and bottom platens of the UTM to uniformly distribute the compression loading on the surfaces. In total eight displacement transducers were attached to record the axial and lateral deformation in each wallette. Four transducers were attached vertically on both faces (two on each face) of the wallette to record the axial deformation. Similarly, four remaining transducers (two on each face) were placed horizontally to record lateral deformation on each face of the wallette. A typical cyclic loading protocol applied to the specimens is shown in Figure 4. The cyclic displacement procedure was taken from the load-displacement responses of the similar wallettes under monotonic testing [20]. The elastic, hardening and peak limits were identified form the load displacement response presented in [20]. The elastic limit point was observed at the one third of the peak load and the hardening limit was considered as 0.8 times the peak load. The number of cycles within each limit are reported in the Table 3.

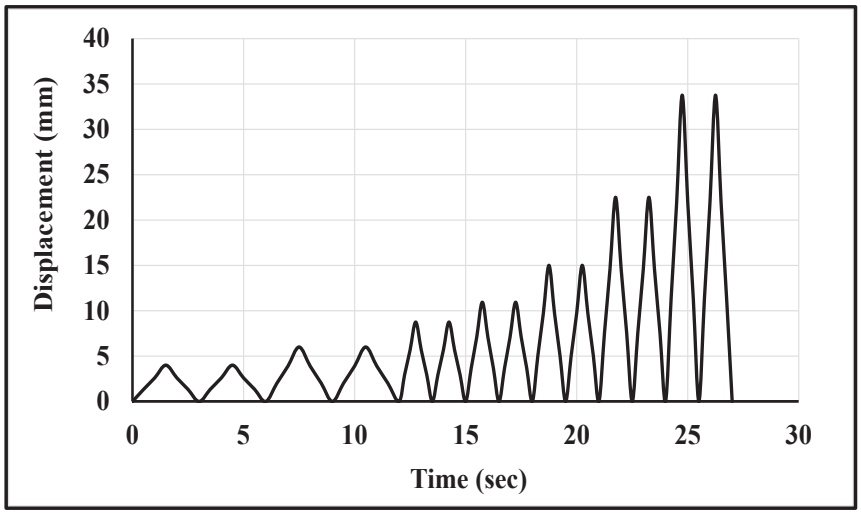

Figure 4: Loading input for the cyclic test of the wallettes

Monotonic Loading	Cyclic Loading	
Load-Displacement Response	**Number of Steps**	**Number of Cycles**
Elastic Limit (one third of peak load)	4 steps	2 cycles at each step
Hardening Limit (0.8 times the peak load)	4 Steps	2 cycles at each step
Peak Limit	3 Steps	2 cycles at each step

Table 3: Typical Cyclic loading protocol

3.2 Failure modes

The failure modes of single, double and triple brick thick bonded brickwork models are shown in Figure 5 in terms of principal strain. The failure pattern observed in the numerical model for all wallettes was in close agreement with the experimental failure modes as shown in Figure 5. For single brickwork wallette, vertical cracks developed in the bricks, mainly on the central area and near the edges of the faces at about 50 to 70% of the peak force. After the peak load, these cracks propagated diagonally and opened leading to the spalling from the edges of the wallettes. However, for the double and triple brick wallettes, a single splitting crack through the thickness of the wallettes and the parallel tensile cracks were observed along the width of the wallettes. During the post-peak stage, the cyclic loading resulted in the wider crack propagation within small span of time associated with the spalling of brick-and-mortar pieces.

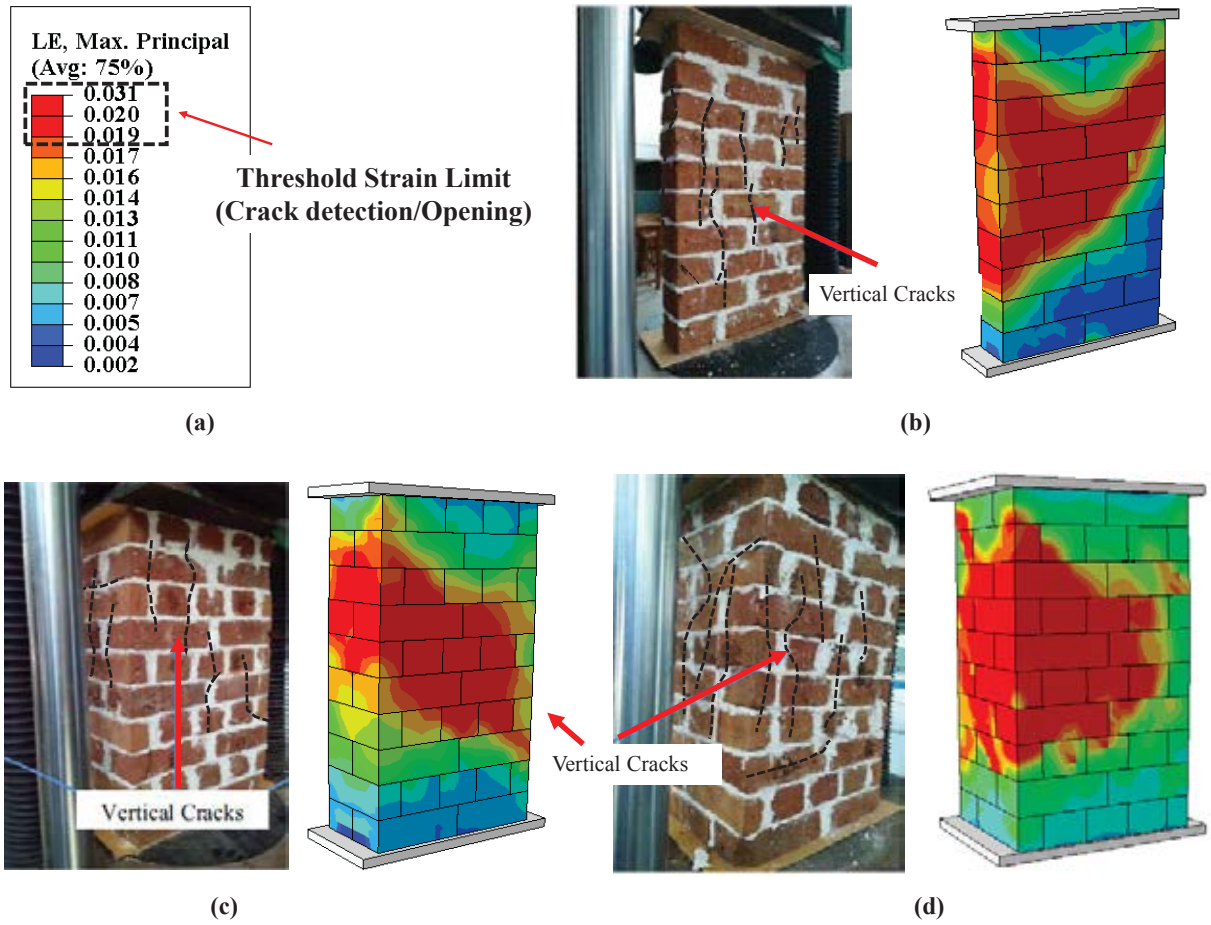

Figure 5: Numerical Failure modes of the brick wallettes: (a) Maximum Strain contour (b) Single brick (c) Double brick and (c) Triple brick

3.3 Stress-strain relationship

Figure 6 shows the compressive strength of single, double and triple brick thick bonded brickwork models under cyclic compression loading. The compressive strength predicted by the FE model of all three brickwork specimens matched well with the experimental data with only 5~10% approx. deviation. The experimental and numerical results show a 10% increase in the compressive strength of the double brick thick brickwork compared to the single- brick wallette. The marginal increase in the compressive strength can be attributed to the reduction in the slenderness ratio (height-to-thickness ratio). However, no significant enhancement in the compressive strength observed when compared double brick to triple brick wallettes. The reason for not increasing the compressive strength is the increase in the number of weak joints (more perpend joint) with the increase in the thickness of the wallettes.

Additionally, it was also observed that the compressive strength for the cyclic loading was lower than for the monotonic loading [20]. The compressive strength reduction observed in the cyclically loaded wallettes was mainly because of the accumulating lateral tractions and inelastic strains in the bonded brickwork. Hence, the accumulation of the strain over time history is significant for the compressive strength of the bonded brickworks as well as for defining the mitigating strategies under cyclic loading.

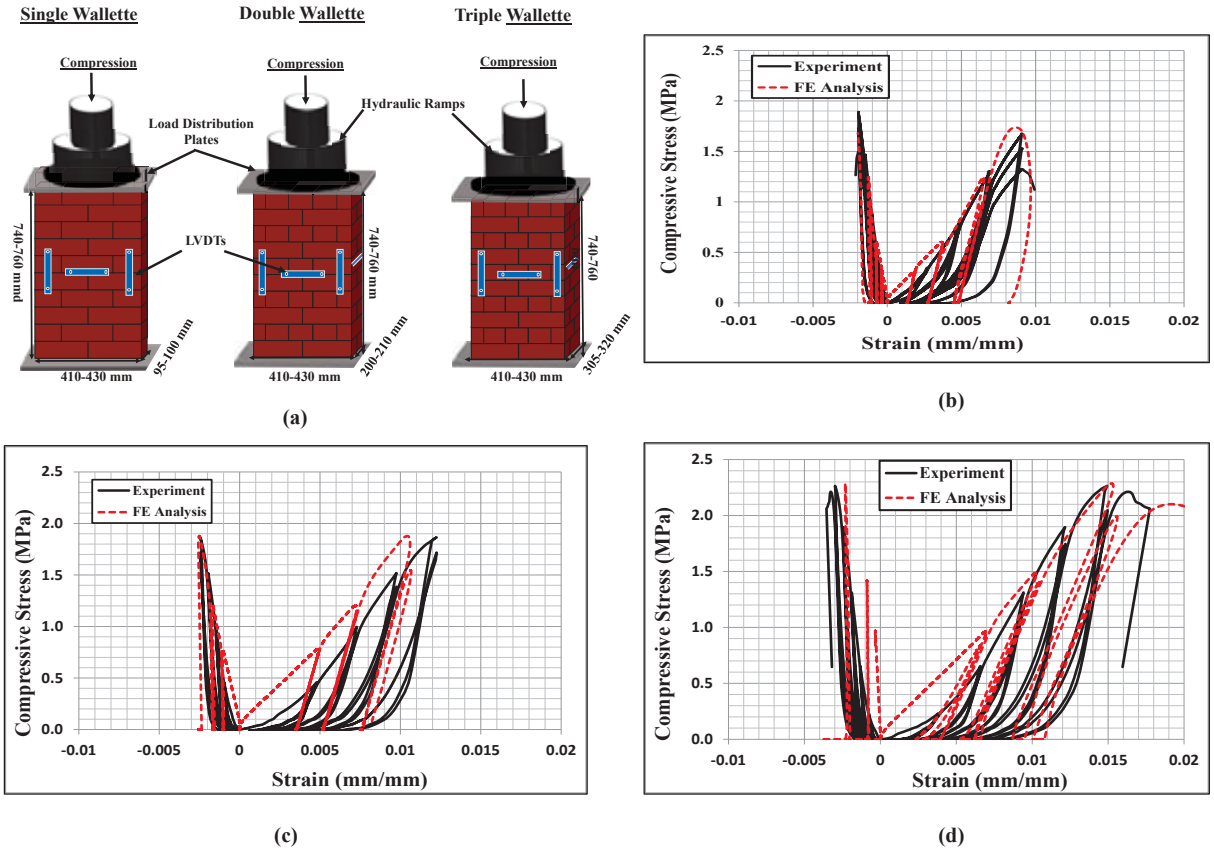

Figure 6: Stress-strain variation of the bonded brick wallettes (a) Experimental setup (b) Single brick (c) Double brick and (d) Triple brick

4 CONCLUSION

A simplified 3D finite element model incorporating expanded bricks with zero thickness cohesive interfaces, representing brick – mortar joints, has been developed for predicting the cyclic compression behaviour of different thicknesses of bonded brick masonry wallettes. The experimental results of bonded brickwork constructed with single, double and triple brick thickness were used for validating the developed model. The FE prediction of the failure modes and cyclic stress-strain curves under the cyclic loading matched well with the experimental results. The change in the thickness of the brickwork samples did not significantly alter the failure pattern of the bonded brickwork confirming the experimental findings that the effect of increase in the thickness of the bonded brickwork (or decrease in the slenderness) was insignificant on the compressive strength of the bonded brickwork.

5 REFERENCES

[1] Sassoni E, Mazzotti C, Pagliai G. Comparison between experimental methods for evaluating the compressive strength of existing masonry buildings. Construction and Building Materials. 2014;68:206-19.
[2] Drougkas A, Roca P, Molins C. Numerical prediction of the behavior, strength and elasticity of masonry in compression. Engineering Structures. 2015;90:15-28.
[3] Zahra T, Dhanasekar M. Prediction of masonry compressive behaviour using a damage mechanics inspired modelling method. Construction and Building Materials. 2016;109:128-38.

[4] Ferretti D. Dimensional analysis and calibration of a power model for compressive strength of solid-clay-brick masonry. Engineering Structures. 2020;205:110064.
[5] Celarec D, Ricci P, Dolšek M. The sensitivity of seismic response parameters to the uncertain modelling variables of masonry-infilled reinforced concrete frames. Engineering Structures. 2012;35:165-77.
[6] Cavaleri L, Di Trapani F. Cyclic response of masonry infilled RC frames: Experimental results and simplified modeling. Soil Dynamics and Earthquake Engineering. 2014;65:224-42.
[7] AlShebani MM, Sinha S. Stress-strain characteristics of brick masonry under uniaxial cyclic loading. Journal of Structural Engineering. 1999;125:600-4.
[8] Oliveira DV, Lourenço PB, Roca P. Cyclic behaviour of stone and brick masonry under uniaxial compressive loading. Materials and structures. 2006;39:247-57.
[9] Facconi L, Minelli F, Vecchio FJ. Predicting uniaxial cyclic compressive behavior of brick masonry: New analytical model. Journal of Structural Engineering. 2018;144:04017213.
[10] Crisafulli FJ. Seismic behaviour of reinforced concrete structures with masonry infills. 1997.
[11] La Mendola L, Papia M. General stress-strain model for concrete or masonry response under uniaxial cyclic compression. Structural engineering and mechanics: An international journal. 2002;14:435-54.
[12] Sima JF, Roca P, Molins C. Nonlinear response of masonry wall structures subjected to cyclic and dynamic loading. Engineering Structures. 2011;33:1955-65.
[13] Thamboo J, Bandara J, Perera S, Navaratnam S, Poologanathan K, Corradi M. Experimental and Analytical Study of Masonry Subjected to Uniaxial Cyclic Compression. Materials. 2020;13:4505.
[14] Zucchini A, Lourenço PB. A micro-mechanical model for the homogenisation of masonry. International Journal of solids and structures. 2002;39:3233-55.
[15] Milani G, Lourenço PB, Tralli A. Homogenised limit analysis of masonry walls, Part II: Structural examples. Computers & Structures. 2006;84:181-95.
[16] Zahra T, Jelvehpour A, Thamboo JA, Dhanasekar M. Interfacial transition zone modelling for characterisation of masonry under biaxial stresses. Construction and Building Materials. 2020;249:118735.
[17] Zahra T, Asad M, Thamboo J. Effect of geometry on the compression characteristics of bonded brickwork. Structures. 2021.
[18] Abasi A, Hassanli R, Vincent T, Manalo A. Influence of prism geometry on the compressive strength of concrete masonry. Construction and Building Materials. 2020;264:120182.
[19] Bolhassani M, Hamid AA, Lau AC, Moon F. Simplified micro modeling of partially grouted masonry assemblages. Construction and Building Materials. 2015;83:159-73.
[20] Thamboo J, Dhanasekar M. Assessment of the characteristics of lime mortar bonded brickwork wallettes under monotonic and cyclic compression. Construction and Building Materials. 2020;261:120003.
[21] Jankowiak T, Lodygowski T. Identification of parameters of concrete damage plasticity constitutive model. Foundations of civil and environmental engineering. 2005;6:53-69.
[22] Asad M, Dhanasekar M, Zahra T, Thambiratnam D. Characterisation of polymer cement mortar composites containing carbon fibre or auxetic fabric overlays and inserts under flexure. Construction and Building Materials. 2019;224:863-79.
[23] Benzeggagh ML, Kenane M. Measurement of mixed-mode delamination fracture toughness of unidirectional glass/epoxy composites with mixed-mode bending apparatus. Composites Science and Technology. 1996;56:439-49.